Global Biogeochemical Cycles

RESEARCH ARTICLE

10.1029/2019GB006223

Key Points:

- Internal organic matter breakdown drives dissolution of the aragonite shells of dead pteropods
- As pteropod decay time progresses, shell dissolution increases
- Postmortem decay is a stronger driver of shell dissolution than aragonite saturation of seawater

Supporting Information:

- Supporting Information S1
- Table S1
- Table S2

Correspondence to:
R. L. Oakes,
roakes@drexel.edu

Citation:
Oakes, R. L., Peck, V. L., Manno, C., & Bralower, T. J. (2019). Degradation of Internal Organic Matter Is the Main Control on Pteropod Shell Dissolution After Death. *Global Biogeochemical Cycles*, *33*, 749–760. https://doi.org/10.1029/2019GB006223

Received 14 MAR 2019
Accepted 24 APR 2019
Accepted article online 6 MAY 2019
Published online 26 JUN 2019

Degradation of Internal Organic Matter is the Main Control on Pteropod Shell Dissolution After Death

R. L. Oakes[1,2], V. L. Peck[3], C. Manno[3], and T. J. Bralower[1]

[1]Department of Geosciences, Pennsylvania State University, University Park, PA, USA, [2]Now at Academy of Natural Sciences of Drexel University, Philadelphia, PA, USA, [3]British Antarctic Survey, Cambridge, UK

Abstract The potential for preservation of thecosome pteropods is thought to be largely governed by the chemical stability of their delicate aragonitic shells in seawater. However, sediment trap studies have found that significant carbonate dissolution can occur above the carbonate saturation horizon. Here we present the results from experiments conducted on two cruises to the Scotia Sea to directly test whether the breakdown of the organic pteropod body influences shell dissolution. We find that on the timescales of 3 to 13 days, the oxidation of organic matter within the shells of dead pteropods is a stronger driver of shell dissolution than the aragonite saturation state of seawater. Three to four days after death, shells became milky white and nano scanning electron microscope images reveal smoothing of internal surface features and increased shell porosity, both indicative of aragonite dissolution. These findings have implications for the interpretation of the condition of pteropod shells from sediment traps and the fossil record, as well as for understanding the processes controlling particulate carbonate export from the surface ocean.

1. Introduction

Thecosome pteropods are a group of pelagic molluscs found throughout the world's oceans (Lalli & Gilmer, 1989). Their delicate shells are formed from aragonite, the more soluble form of calcium carbonate than calcite (Lalli & Gilmer, 1989; Mucci, 1983), making them susceptible to dissolution. Consequently, pteropods have been the subjects of many ocean acidification related studies (cf. Manno et al., 2017).

Pteropod shells are visibly altered by dissolution changing from glassy and transparent when pristine to milky-white when dissolved (Almogi-Labin et al., 1986; Gerhardt et al., 2000). Pteropod shell condition has been used to visually assess the extent of shell dissolution in both modern and fossil samples (Gerhardt et al., 2000; Gerhardt & Henrich, 2001). In the modern ocean, the condition of pteropod shells in sediment traps have been used to monitor carbonate chemistry (Meinecke & Wefer, 1990; Mohan et al., 2006), with the notion that shell dissolution is indicative of aragonite undersaturated waters between the sea surface and the depth of the sediment trap (Almogi-Labin et al., 1986; Gerhardt et al., 2000). In the fossil record, shell condition has been used to assess the impact of dissolution on the growth of living pteropods and their subsequent alteration during burial. For example, Wall-Palmer et al. (2012, 2013) used the size and extent of dissolution of pteropod shells to assess the impact of changing atmospheric CO_2 levels over glacial-interglacial cycles on pteropod shell growth in the Caribbean Sea and Gerhardt and Henrich (2001) used pteropod shell dissolution as an indicator of bottom water chemistry in order to track changes in ocean circulation through time.

Reliably applying pteropod shell condition as an indicator of past, present, and future changes in ocean chemistry requires that taphonomic processes affecting shell condition are well understood. In general, the preservation and dissolution of carbonate minerals is largely assumed to be controlled by their chemical stability in seawater (Berger, 1978; Berner et al., 1976; Gerhardt et al., 2000; Gerhardt & Henrich, 2001). This is described by the saturation state (Ω), the ratio between the product of calcium and carbonate ions in seawater and at equilibrium (Broecker & Peng, 1982):

$$\Omega = \frac{\left[Ca^{2+}\right]_{sw} \times \left[CO_3{}^{2-}\right]_{sw}}{\left[Ca^{2+}\right]_{saturation} \times \left[CO_3{}^{2-}\right]_{saturation}}$$

At $\Omega > 1$, water is supersaturated and the carbonate mineral is stable; at $\Omega < 1$, water is undersaturated and carbonate is chemically unstable. Carbonate-bearing sediments are therefore found in shallow and

intermediate waters above the saturation horizon, with aragonite restricted to shallower depths than calcite because of its higher solubility (Mucci, 1983).

Although carbonates are chemically stable above the saturation horizon, a number of studies have found that significant dissolution can occur in these supersaturated waters (Buitenhuis et al., 2019; Manno et al., 2007; Martin & Sayles, 1996; Milliman et al., 1999; Milliman & Droxler, 1996; Schiebel et al., 2007). One potential cause of this dissolution is the breakdown of organic matter by microbes (Milliman et al., 1999; Schiebel, 2002; Schiebel et al., 2007), which releases nutrients and CO_2 into the surrounding waters. Organic matter may clump into marine aggregates while sinking, producing undersaturated microenvironments when it oxidizes (Lohmann, 1995; Milliman et al., 1999). Carbonate in these aggregates could therefore be exposed to undersaturated water causing them to dissolve within an otherwise carbonate supersaturated water column.

In addition to processes occurring in the water column, pteropods have a large mass of internal organic matter. The bodies of pteropods are attached to the inside of the shell in life and their winged foot protrudes from the aperture for locomotion. Upon death, the pteropod retracts its foot, encapsulating the organic body within the shell which, on decay, could cause an undersaturated microenvironment to form within the shell. This makes them ideal test organisms on which to study the relative impact of decaying organic matter on shell condition, which could cause aragonite dissolution to occur above the saturation horizon.

Dissolution has been found in pteropods from sediment traps above the aragonite saturation horizon (Bathmann et al., 1991; Collier et al., 2000; Manno et al., 2007; Roberts et al., 2011). A study of two sediment traps from Terra Nova Bay found the abundance of pteropods dramatically decreased between the shallow trap and the deep trap, both of which were above the aragonite saturation horizon (Manno et al., 2007). Supralysoclinal pteropod shell dissolution has also been documented in two other polar studies (Collier et al., 2000; Roberts et al., 2011), which implies that it is a widespread phenomenon.

Here we conduct two decay experiments on the pteropods *Limacina retroversa* and *Limacina helicina antarctica* to assess the impact of soft body degradation on the dissolution of pteropod shells. This relationship is tested in both ambient seawater and seawater with perturbed aragonite saturation levels. Light and scanning electron microscopy are used to assess shell condition, both internally and externally, and microcomputed tomography (micro-CT) is used to assess shell thickness changes in order to ascertain the relative importance of Ω_{arag} and organic matter degradation on the dissolution of aragonitic pteropod shells.

2. Materials and Methods

This study is based on two experiments. The first, a 3.5-day decay experiment conducted in ambient seawater, is used to solely assess the impact of the decaying pteropod soft body on shell dissolution. The second, a 13-day decay experiment, uses both ambient seawater and seawater with manipulated chemistry to test (1) the impact of the length of decay on shell condition and (2) the relative significance of aragonite saturation and decaying organic matter on the dissolution of pteropod shells after death. The two experiments use the same genus but different species of Limacinid pteropods due to the availability of organisms collected at each site.

2.1. 3.5-Day Decay Experiment Design

Pteropods were collected north west of South Georgia in the Southern Ocean (−53.81174N, −40.11167E) on 8 December 2015 during cruise JR15002 on RRS *James Clark Ross*. Bulk plankton samples were collected using a British Antarctic Survey motion-compensated bongo net with 200-μm mesh deployed to 200 m and hauled vertically at 20 m/min. *Limacina retroversa* were picked from the sample using a wide mouthed plastic pipette and examined and imaged under the light microscope. Only actively swimming specimens were selected for the experiment to ensure accurate determination of the decay period. Pteropods were terminated by rinsing the shells in buffered deionized water (DIW), and specimens were randomly split into two batches of 10 shells: the first batch, used as a control of initial shell condition, was rinsed with buffered DIW and air dried. The second batch was returned to a container of unfiltered seawater and stored in the dark at 4 °C for 3.5 days. After incubation, the pteropods were imaged, rinsed with DIW, and air dried. Samples of sea water were collected from 5-m depth at a nearby site (−52.8116N, −39.9727E) for carbonate chemistry analysis (Table 1; see protocol in section 2.3).

Table 1
Carbonate Chemistry Measurements for the Two Decay Experiments

Seawater target pCO_2	Temperature (°C)	Salinity	pH	Total Alkalinity (mmol/kg)	Total CO_2 (mmol/kg)	pCO_2 (ppm)	Aragonite saturation (Ω_{arag})
3.5-day decay experiment							
Ambient	2.5	33.8	8.1	2,280.54	2,123.98	321	1.77
13-day decay experiment							
Ambient	1.9 ± 0.32	34.1 ± 0.02	8.1 ± 0.02	2,333.12 ± 11.5	2,219.21 ± 19	378 ± 12	1.40 ± 0.11
750 ppm	1.9 ± 0.62	34.1 ± 0.02	7.8 ± 0.01	2,333.12 ± 8.90	2,284.12 ± 08	753 ± 22	0.89 ± 0.04
1200 ppm	1.9 ± 0.65	34.1 ± 0.02	7.6 ± 0.02	2,333.12 ± 9.50	2,297.04 ± 13	1,200 ± 13	0.78 ± 0.09

Note. For the 3.5-day decay experiment, the water measured was collected from 5-m depth. For the 13-day decay experiment, reported values are the mean values of carbonate system parameters of incubated sea water at the beginning and end of the perturbation experiments. The chemistry of the seawater in the 750- and 1,200-ppm conditions in the 13-day decay experiment was adjusted using a combination of Na_2CO_3 and HCl based on the recommendations of Gattuso et al. (2010).

2.2. The 13-Day Decay and Aragonite Saturation Experiment Design

Pteropods were collected south west of South Georgia (−55.19129, −41.34553) on 3 December 2013 during cruise JR291 on RRS *James Clark Ross* using MOCNESS (Multiple Opening/Closing Net and Environmental Sensing System) nets 8 and 9, opened at 100–50 and 50–0 m, respectively. Thirty swimming specimens of *Limacina helicina antarctica* were recovered and terminated by rinsing with DIW. Two hundred fifty milliliter incubation jars were filled with 0.2-μm filtered seawater using a plastic tube from the master tank to the bottom of the incubation jar to minimize exchange of CO_2 with the air. Pteropods were carefully transferred using a wide mouthed pipette into the incubation jars, which were subsequently sealed without any air in the head space.

Decay experiments were run at three conditions: $\Omega_{arag} = 1.40$ (filtered seawater and ambient CO_2), $\Omega_{arag} = 0.89$ (750 ppm CO_2), and $\Omega_{arag} = 0.78$ (1,200 ppm CO_2; Table 1). Ambient seawater was adjusted using Na_2CO_3 and HCl (Gattuso et al., 2010) to alter the pH while maintaining the total alkalinity (TA; Table 1). The acid and base additions were calculated using the seacarb software (Lavigne et al., 2011) with pH and TA as inputs. pH was measured directly using a pH electrode (Metrohn 826, MERK standards solution, NBS). The initial TA of seawater was estimated using a regionally refined surface salinity and temperature algorithm using underway samples taken on cruise JR274 to the Scotia Sea (Tynan et al., 2016):

$$TA = 683.41S - 9.139S^2 - 1.37T - 0.896T^2 - 10364.16$$

where S is surface salinity and T is surface temperature in degrees celsius (M. P. Humphreys, 23rd May 2018, personal communication). This algorithm was used as it was found to replicate measured TA values better at low and high salinities than the previously published algorithm from this region (Lee et al., 2006). When checked against 366 measured values from the region (sample location ±10° latitude and longitude) downloaded from the GLODAPv2 database (Olsen et al., 2016), the algorithm underestimated TA by 2.7% and the data had a standard deviation of 12.3 μmol/kg. The TA of the adjusted seawater was later analysed in the laboratory (see section 2.3).

Experiments were maintained in the dark at between 1.8 and 2.2 °C for 13 days. At the end of the experiments, pteropods were imaged, rinsed in DIW, and air dried. Subsamples of the water from each experiment were taken at the start and end of each decay experiment.

2.3. Carbonate Chemistry Analysis

In both decay experiments, subsamples of seawater were fixed with 2% mercuric chloride for subsequent shore-based carbonate chemistry analyses. The TA and dissolved inorganic carbon (DIC) of each sample were measured simultaneously by a potometric titration system following the methods of Edmond (1970), with a closed cell described by Goyet et al. (1991). The accuracy (3 mmol/kg for TA and 4 mmol/kg for DIC) was determined by analyzing certified reference material with known TA and DIC concentrations. Aragonite saturation (Ω_{arag}) was indirectly calculated from TA and DIC using the CO2SYS software (Pierrot et al., 2006) with carbonate dissociation constants by Mehrbach et al. (1973) refitted by Dickson (1990). All the carbonate chemistry parameters are given in Table 1.

2.4. Imaging

All specimens were imaged post-cruise in the Paleobotany Laboratory at The Pennsylvania State University. Pteropods were positioned in the apical view on pieces of nitrile glove for stability during imaging. Images were captured using a Nikon SMZ-1500 stereoscope and a Nikon NI-150 high intensity illuminator light source, a Nikon DS-Ri1 camera, and *Nikon NIS Elements v. 3* software. Between 10 and 15 images were taken per specimen to capture the full topographic range of the shell. Images were stacked using the *PMax* function in *Zerene Stacker v. 1.04* to build a composite, focused image with a resolution of 4,076 × 3,116 pixels.

Two specimens from the 3.5-day experiment, and each of the 13-day experimental conditions were imaged using nano-scanning electron microscope (SEM). Samples were coated with an 8-nm layer of iridium and imaged on the FEI Nova 630 field emission SEM in the Materials Characterization Laboratory at The Pennsylvania State University. Shells were mechanically broken with a steel spike, and the fragments removed with a paintbrush so the internal face could be imaged. The shells were then recoated with iridium before imaging.

2.5. Shell Condition

Shell condition was analyzed using opacity measurements following the methods of Bergan et al. (2017). Briefly, shells were imaged in the apical view, stabilized on pieces of nitrile glove, and illuminated with an oblique light source. A white balance calibration was performed before taking each image. Using *ImageJ* (Schneider et al., 2012), shell material was manually selected, avoiding any organic matter (brown or black, usually in the innermost whorls of the shell) or oversaturated areas where the light had been reflected straight back from the shell (see Oakes et al., 2019 for more details). The *measure* tool was used to find the average greyscale value of the selected shell area and divided by 255 (the maximum greyscale value). The background was also assessed using the same method, avoiding any shadows. The shell opacity is calculated as the difference between the shell value and the background value, which normalizes for any lighting variability.

2.6. Micro-CT Scans

A subset of five randomly selected specimens from each of the experimental conditions in the 13-day decay experiments were imaged in a micro-CT scanner at *GE Inspection Technologies, Lewistown, PA*. Individual specimens were scanned at 65 kV and 230 μA for 52 min using a *GE phoenix vtome|x|m* with a 180-kV microfocus tube and a GE DXR detector. Data were reconstructed using *GE datos|x version 2* and processed using *VG Studio Max 2.2.3* and *Avizo 9.1*. Shell thickness maps were created using the *BoneJ* plugin for *ImageJ* (Doube et al., 2010; Hildebrand & Rüegsegger, 1997) and visualized using *Avizo 9.1*. These data were translated into whole shell thickness histograms using the *Histogram* tool in *Avizo 9.1*.

A sample set of five specimens for each sample could be considered a relatively low number from which to draw conclusions. Given the prohibitive costs of CT scans, we sought to optimize the number of scans required to provide robust results and satisfy financial constraints. We ran a test to assess the impact of the number of scans on the standard deviation of modal shell thickness of a sample set. We performed a bootstrap-resampling analysis on a separate data set where 13 Scotia Sea *Limacina retroversa* specimens, with similar shell diameter distribution to specimens within this study, were CT scanned. We sampled this data set, with replacement, at sample sizes of 3 to 13. We found that the mean modal shell thickness was highly reproducible (Text S1 and Figure S1 in the supporting information). Given the reproducibility of these measurements, we are satisfied that a sample size of five specimens per sample for this study will enable us to derive meaningful conclusions relating to shell thickness variability between treatments. More details of this test are given in the supporting information (Text S1 and Figure S1).

3. Results

3.1. 3.5-Day Decay Experiment

The shells of control specimens of *Limacina retroversa*, preserved (dried) at the time of collection, are consistently glassy and pristine (Figures 1a, 1c, and 1d), whereas the shells of specimens left to decay in ambient seawater (supersaturated with respect to aragonite) for 3.5 days are consistently cloudy and white (Figures 1b, 1e, and 1f). It is important to note that a similar shell surface sheen is common to all specimens imaged under the light microscope (Figures 1c–1f). Opacity measurements show that over the 3.5-day time

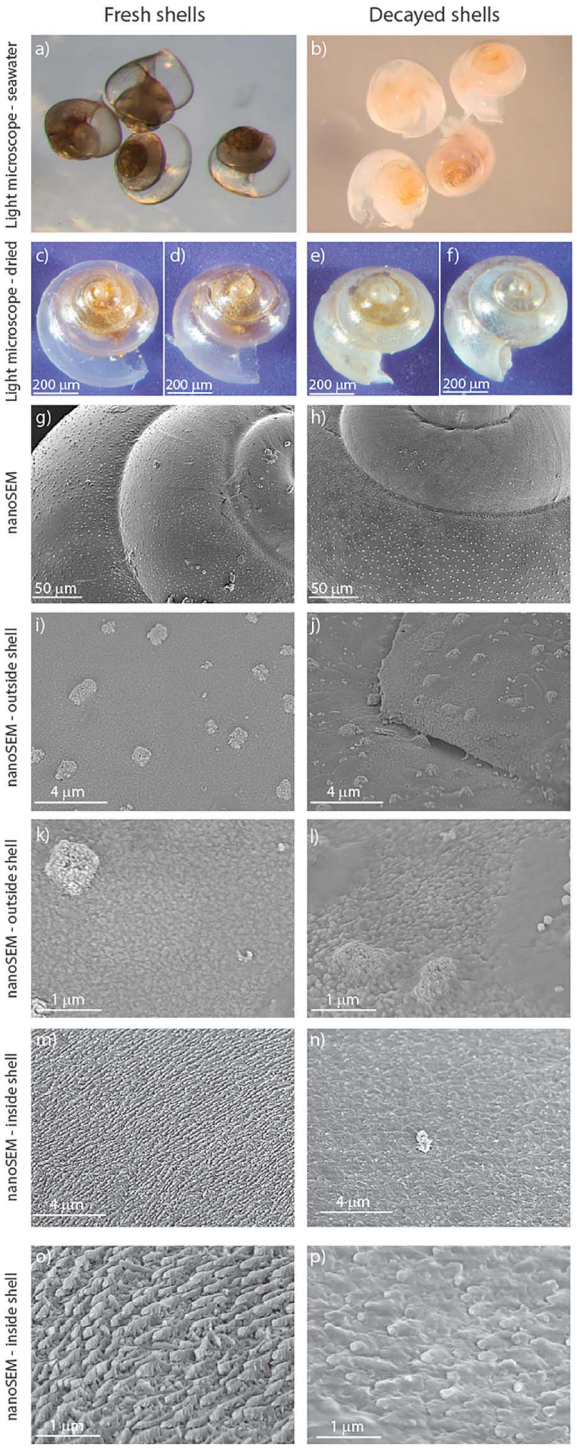

Figure 1. A comparison of shell degradation between specimens of *L. retroversa* preserved immediately after collection (a, c, d, g, i, k, m, and o), and *L. retroversa* left to decay for 3.5 days after termination (b, e, f, h, j, l, n, and p). Images in the two columns are paired, enabling features to be compared at the same scale. When pristine, shells are glassy (a, c, and d), and when decayed, they turn cloudy white (b, e, and f). The external surfaces look similar between the fresh and decayed shells (g–l) with both living and dead specimens retaining surface sheen (c–f); however, the internal surfaces look different, with fresh shells having considerably more surface texture (~0.5 µm; m, o) than the dead shells (n, p).

period, shells had been altered from an opacity of 0.19 ± 0.02 to 0.33 ± 0.02 (Figure 2). Nano-SEM images reveal that the outer surfaces of the fresh and decayed shells have all experienced a similar amount of degradation (Figures 1g–1l); however, the inner shell walls of the control and decayed shells look distinctly different (Figures 1m–1p). The shells of control specimens have a rough internal surface, caused by the intersection of the ends of the crossed-lamellar aragonite crystals, which form the innermost layer of the shell, with the internal surface (Figures 1m and 1o). Decayed shells have a smoother internal surface, indicating that this surface has been modified (Figures 1n and 1p).

3.2. 13-Day Decay Experiment

All external surfaces of shells of 13-day decayed *L. helicina antarctica* incubated under three different levels of aragonite saturation look remarkably similar: milky white with surface sheen under the light microscope and uniform surface etching visible on the outer wall in SEM images (Figures 3 and S2). Opacity measurements for the three incubated treatments range from 0.50–0.57 and do not vary with aragonite saturation (Figure 2). Shells incubated in ambient seawater for 13-days have higher opacity values than specimens from the 3.5-day decay experiment (0.52 versus 0.33; Figure 2). Images from the SEM analysis highlight the same trend of shell condition deteriorating with increased duration of organic matter decay (i.e., 3.5-day decay experiment versus 13-day decay). This implies that organic matter degradation plays a greater role in shell dissolution than the aragonite saturation of the surrounding seawater (Figures 1, 3, and S2). In all shells from the 13-day decay experiment, the outermost, organic bound layer of aragonite exhibits uniform dissolution, with individual crystals of the underlying prismatic aragonite layer visible under SEM (Figures 3 and S2).

Similar to the 3.5-day decay experiment conducted on *L. retroversa*, the internal shell surface of the control and dead incubated *L. helicina antarctica* look distinctly different: the control specimens have a rough internal surface (Figures 4a–4c), whereas the decayed pteropods have a smooth internal surface, where surface features have been altered (Figures 4d–4f).

SEM images of cross sections through the shells from the control and the 13-day decay experiment corroborate the trends in shell deterioration observed in light microscope and surface SEM images (Figure 5). The shell from the control exhibit three distinct layers from outside to inside: organic, prismatic, and crossed lamellar (Sato-Okoshi et al., 2010; Figure 5a). In the shells of 13-day decayed *L. helicina antarctica* specimens, these three layers are less distinguishable as the crystal structure appears to have become disordered. The innermost crossed-lamellar layer in particular seems to have increased in porosity indicating that a considerable amount of aragonite has been removed (Figure 5b).

Despite the removal of shell material associated with the dissolution of internal features and the increase in porosity, there was little change in overall shell thickness. Whole shell thickness histograms show that there is less than 1-µm decrease in modal shell thickness between the control specimens and the *L. helicina antarctica* shells in the two other 13-day decay treatments (Figure 6). The majority of aragonite loss during dissolution is therefore manifested as a decrease in shell density as opposed to shell thinning (Figures 5 and 6).

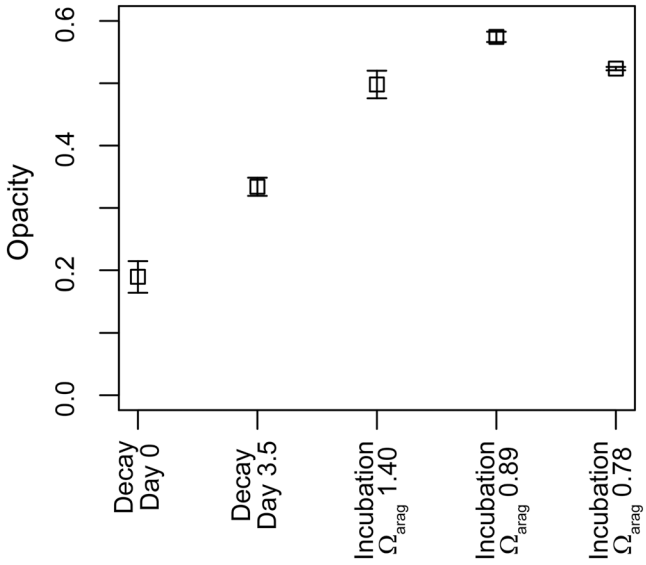

Figure 2. Changes in shell opacity through the 3.5-day and the 13-day decay experiments. Shell opacity increases in samples preserved in supersaturated water as the length of time the sample has been decaying increases. There is no trend between opacity and aragonite saturation. Error bars = ±1 standard deviation. Raw data are available in Table S1.

4. Discussion

The shells of dead pteropods were visibly altered in both the 3.5-day (*L. retroversa*) and 13-day (*L. helicina antarctica*) decay experiments, changing from pristine and glassy to cloudy and white as they decayed (Figures 1a–1f, 2, and 3). The opacity of shells in ambient seawater, saturated with respect to aragonite (Ω_{arag} = 1.77 and 1.40 for the 3.5-day and the 13-day decay experiments, respectively), increased from control specimens to specimens which had decayed for 3.5 and 13 days (Figure 2). The shell opacities of the *L. helicina antarctica* specimens did not increase with decreasing aragonite saturation during the 13-day decay experiment as anticipated (Bednaršek et al., 2014; Figure 2). We therefore conclude that the duration of the decay of the pteropod's body has a larger control on shell condition than the aragonite saturation of the surrounding seawater and that saturation state is not the primary driver of dissolution in recently dead specimens.

4.1. External Shell Dissolution

The established view of biogenic calcium carbonate stability in seawater predicts rates of dissolution will increase as saturation state decreases (Berger, 1978; Berner et al., 1976; Cubillas et al., 2005; Gerhardt & Henrich, 2001). However, SEM images of the external surface of *L. helicina antarctica* shells from the 13-day decay experiment consistently show comparable levels of dissolution at the three different aragonite saturation states (Figures 3 and S2). Although the values for aragonite saturation were varied, the role of decaying organic matter incorporated in marine snow was not simulated in these decay experiments. These undersaturated microenvironments could play an additional role in external shell degradation in the natural system.

Pteropods have an ultrathin periostracum, an impermeable organic coating that covers the outside of the shell, protecting the aragonitic layers from the surrounding seawater (Peck, Tarling, Manno, Harper, & Tynan, 2016; Peck, Tarling, Manno, & Harper, 2016; Sato-Okoshi et al., 2010). Formed from sclerotinized protein (Harper, 1997), the periostracum has been shown to remain intact after death (Tunnicliffe et al., 2009). In the specimens in this study, the presence of the periostracum is evident in our specimens by the persistent surface sheen observed on both the control and decayed specimens (Figures 1 and 3). The persistent presence of the periostracum implies that its protective role does not stop immediately after death but continues to form a barrier on the outer shell wall. As such, dead specimens exposed to waters that are undersaturated with respect to aragonite show the same levels of dissolution on their outer wall as all those in water saturated with respect to aragonite, and all specimens exhibit lower dissolution rates that are predicted from nonorganically bound aragonite (Cubillas et al., 2005). With dissolution from the external surface of the shell restricted, we hypothesize that internal rather than external saturation state change controls pteropod shell degradation after the organism dies.

4.2. Internal Shell Dissolution

Pteropods have a high body to shell ratio. Haddad and Droxler (1996) first suggested that the oxidation of this organic body causes pteropod shells to become cloudy postmortem and this has since been supported by Peck, Tarling, Manno, Harper, and Tynan (2016). If postmortem shell dissolution results from aragonite undersaturation inside the shell, there should be evidence of dissolution on the internal shell surface.

Nano-SEM analysis reveals consistent differences between the internal structure of living and dead, decaying pteropods (Figures 1 and 4). Control specimens of both *L. retroversa* and *L. helicina antarctica* have an irregular internal surface, likely caused by the intersection between the internal surface and the exposed terminations of the aragonite crystals in the crossed-lamellar layer (Grégorie, 1972; Sato-Okoshi et al., 2010; Figures 1, 4, and 5). These internal terminations have different morphologies in the different species (Grégorie, 1972); crystals are more needle-like in *L. helicina antarctica* (Figure 1) and are broader in *L. retroversa* (Figure 4). However, in decayed pteropods of both species, the internal surface appears much smoother

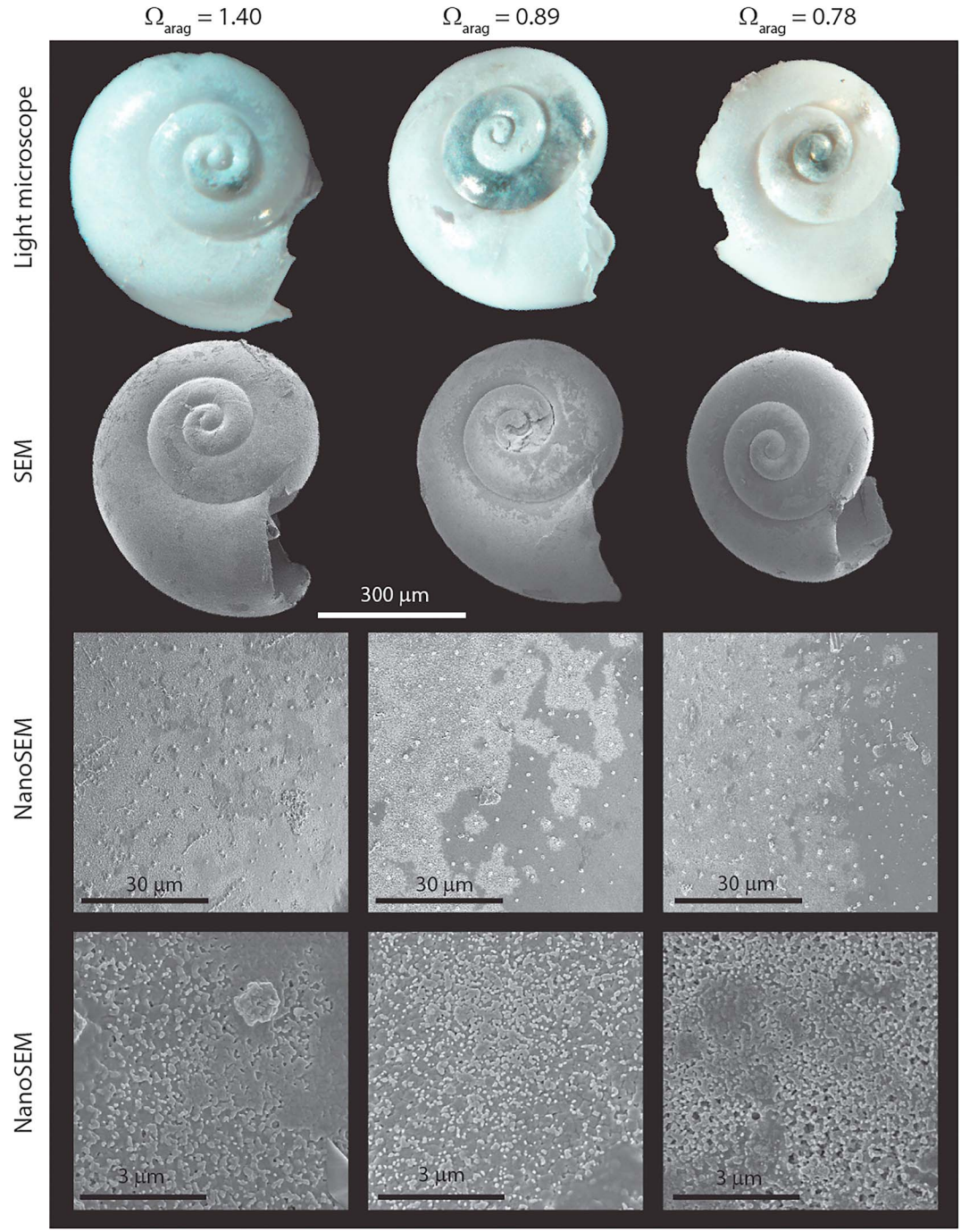

Figure 3. Comparing changes in external shell degradation with decreasing aragonite saturation in specimens of *Limacina helicina antarctica* from the 13-day decay experiment. Shell breakage occurred during sample preparation and therefore should not be considered as a signal of shell degradation. We predicted that there would be significant deterioration in the condition of the shell exterior with decreasing seawater aragonite saturation state; however, the surface features appear to be remarkably similar, with only a slight increase in dissolution at lower saturations. Additional images can be seen in Figure S2.

(Figures 1 and 4) suggesting that dissolution, or a combination of dissolution and reprecipitation, has occurred at the internal surface. Comparable dissolution of shell material resulting from the degradation of organic material within a shell has been observed in dead mussels at hydrothermal vents (Tunnicliffe et al., 2009), and in bivalve shells with elevated levels of pCO_2 in the extrapallial fluid (Melzner et al.,

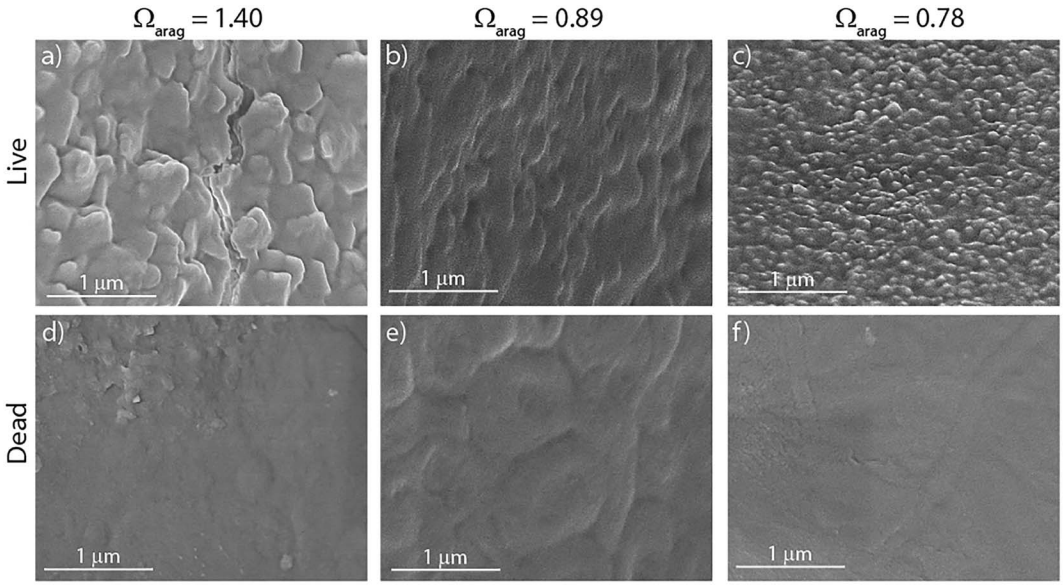

Figure 4. Nanoscanning electron microscope images of the internal shell surface a live *L. helicina antarctica* and decayed *L. helicina antarctica* from the 13-day decay experiment. The shells of the living organisms have significant topography, caused by the intersection of the crossed-lamellar aragonite crystals with the internal surface (Figure 5). This surface topography is ~ 0.5 µm in height. In the decayed shells, this surface topography has been removed likely due to the low saturation conditions associated with the decomposition of the organic pteropod body after death. This indicates that at least 0.5 µm of material has been dissolved away from the internal surface of the shell.

2011). The combination of dissolution and reprecipitation has been proposed to occur inside the tests of planktonic foraminifera as they fall through the water column (Schiebel et al., 2007).

Cross sections through the shells of control and 13-day decayed *L. helicina antarctica* specimens show that although the shell of the decayed specimen maintains its overall form, there is an increase in the porosity of the shell wall with degradation, especially in the crossed-lamellar layer (Figure 5). Our observations indicate that aragonite undersaturated water, generated from the decay of the organic pteropod body, has been able to make direct contact with the aragonite through the inner shell surface leading to dissolution of the

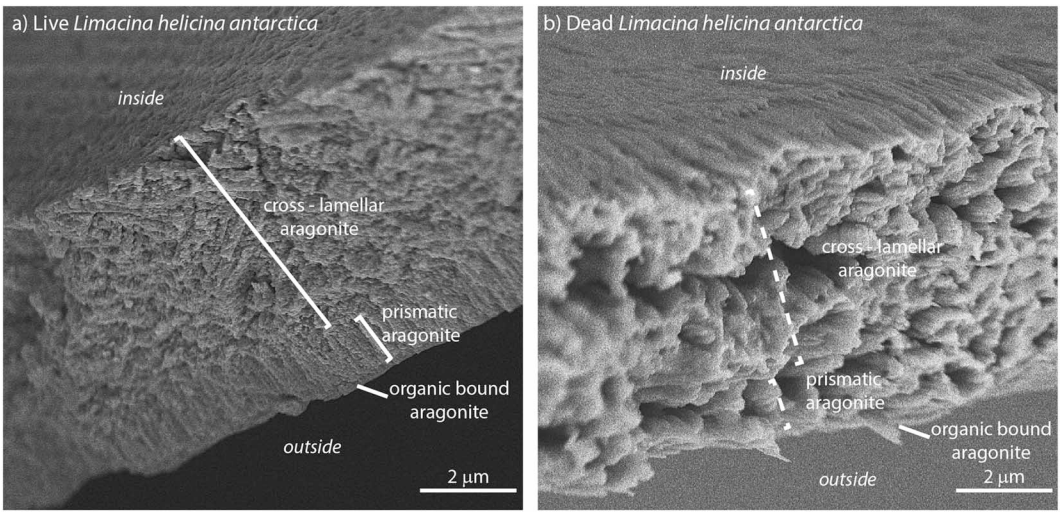

Figure 5. (a, b) A cross section through a live and a decayed shell of *Limacina helicina antarctica from the 13-day decay experiment* observed in nanoscanning electron microscope. Shells were sectioned using an ion mill. The cross sections show three layers of aragonite which, from outside to inside are organic bound, prismatic and crossed lamellar. In the fresh shell, where the crossed-lamellar crystals intersect with the internal surface, it creates a rough surface. However, this has been removed in the decayed shell. The structure of the decayed shell has begun to collapse, increasing the internal porosity of shell, which is especially noticeable in the crossed-lamellar layer.

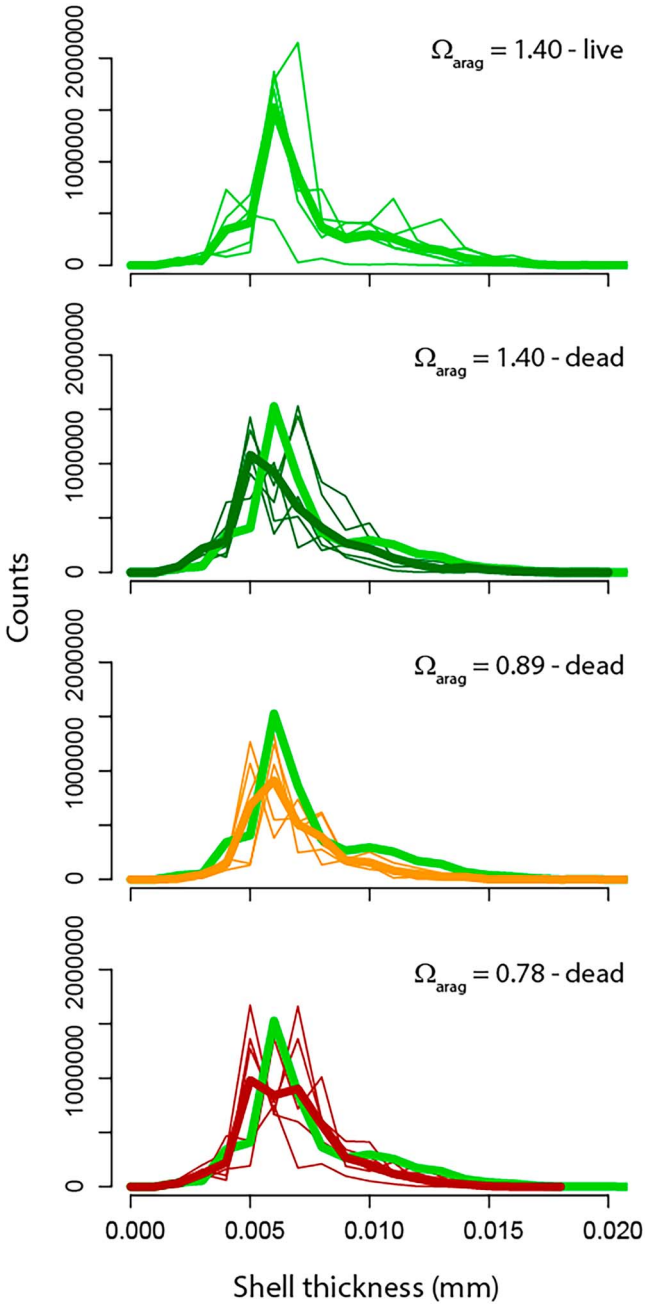

Figure 6. Stacked plots to assess how dissolution varies between live and decayed shells of *Limacina helicina antarctica* and between shells of *Limacina helicina antarctica* incubated for 13-days in water increasingly undersaturated with respect to aragonite. Graphs are whole shell thickness histograms created from computed tomography scan data; thin lines represent individual specimens, and thick lines represent the sample average. The average line for the live specimens from ambient seawater is added to each graph for comparison. Although there is variability among specimens, likely due to differences in the initial thickness of the shell, the average shell thickness is not significantly different in the four treatments. Despite the minimal shell thinning reported here, the loss of carbonate is clearly evident in scanning electron microscope cross sections of the shell wall (Figure 5). Raw data are available in Table S2.

aragonite crystals. The internal crossed-lamellar layer is more porous than the outer prismatic layer (Figure 5) consistent with the hypothesis that dissolution is being initiated from the inside of the shell.

Despite considerable dissolution of aragonite, the shell structure remains intact and held together by the refractory conchiolin matrix, the protein rich, organic framework onto which gastropods precipitate their shells (Crenshaw, 1990; Grégorie, 1972). The effectiveness of this organic matrix in maintaining the structural integrity of the shell is supported by whole shell thickness measurements from CT scan data, which show that despite extensive dissolution, the overall shell thickness does not change significantly (Figures 5 and 6). Despite minimal shell thinning, the loss of carbonate is clearly evident by the increased porosity of the shell wall (Figure 5).

The original topography on the internal shell wall created by the protruding crossed-lamellar crystals has a height of ~0.5 μm in both species (Figures 1m–1p and 4). Loss of this topography in the decayed specimens indicates that shells thinned by at least 0.5 μm and a loss of approximately 10 % of the total shell carbonate (Table S3). The true magnitude of carbonate loss is considerably greater than this due to the increased porosity of the crossed-lamellar layer in the decayed shell relative to the original shell (Figure 5). Unfortunately, the density of the pteropod shell material cannot be quantified from the CT scans. Although grayscale values of CT data can be used to determine density (e.g., in human body scans), because of the thickness of the shells measured here (~8-μm modal shell thickness) and the voxel size at which they were scanned (1–2 μm^3), edge effects are too large to enable accurate quantification.

4.3. Implications for Interpretation of Sediment Trap and Fossil Records

Based on the observed changes in the condition of pteropod shells during decay, we find that the postmortem oxidation of internal organic matter impacts pteropod shell dissolution more than the saturation state of seawater. This dissolution of carbonate, even within a saturated water column, could account for some of the loss of particulate carbonate from above the saturation horizon as reported in sediment trap studies (e.g., Milliman et al., 1999).

4.3.1. Sediment Trap Records

The condition of pteropod shells collected in sediment traps has been used to make inferences about the carbonate chemistry of seawater through time (Manno et al., 2007; Roberts et al., 2011). Dead pteropods sink through the water column at ~0.5 cm/s (Lalli & Gilmer, 1989). Based on these rates, it would take ~2.3 days to fall 1,000 m and 3.5 days, the length of our shorter decay experiment, to fall 1,500 m. The changes in shell condition observed in our 3.5-day experiment are therefore likely to be comparable to the postmortem changes expected to occur in the shells of dead pteropods, which enter sediment traps and shallow marine deposits before predation (i.e., with their bodies still inside the shell).

A sediment trap study from the Norwegian Sea found that the organic bodies of pteropods degraded with depth with partial degradation by 250 m and complete degradation by 1,000 m (Bathmann et al., 1991), and a recent modeling study found that observations of aragonite export could only be reproduced using a model which inferred substantial dissolution above the saturation horizon (Buitenhuis et al., 2019). The findings

from this study suggest that organic matter degradation is likely driving dissolution of the shell in the depth ranges sampled by sediment traps.

4.3.2. Fossil Record

Pteropods are found in the fossil record from the Early Eocene to the present, with possible specimens spanning back into the Cretaceous (Janssen, 2012; Janssen et al., 2011, 2016; Janssen & Peijnenburg, 2017). Because of their mineralogy, pteropod shells are often diagenetically altered, limiting their use in palaeoceanographic studies (Manno et al., 2017). Pteropod preservation in the fossil record is interpreted to be controlled by Ω_{arag} in the surface ocean (Wall-Palmer et al., 2012) and at the sediment-water interface (Berger, 1978; Berner et al., 1976; Gerhardt et al., 2000; Gerhardt & Henrich, 2001). Based on the results of this study, we postulate that the organic matter content of the water column and sediments at the seafloor may have a large influence on the preservation potential of pteropod shells in the fossil record (Almogi-Labin et al., 1986). Our results do not preclude the application of pteropod-based proxies in evaluating past changes in ocean circulation, temperature, and the depth of the saturation horizon (Gerhardt & Henrich, 2001; Keul et al., 2017; Wall-Palmer et al., 2013); however, the condition of the pteropod shells and the impact of taphonomic changes should be evaluated before these methods are applied.

4.4. Next Steps

The results of these decay experiments highlight the importance of considering the impact of degradation of internal organic matter when interpreting pteropod shell condition. To develop our understanding of postmortem processes on shell condition, we suggest that future studies consider the following: (1) conducting decay experiments for longer durations; (2) determining the impact of additional organic matter, such as would be found when the shell were incorporated within a fecal pellet or marine snow aggregate; and (3) assessing another species of pteropod to see if the relationships between organic matter decay, aragonite saturation, and shell degradation observed in this experiment are consistent across species. Finally, although this investigation focused on pteropods, which are highly susceptible to dissolution because of their aragonitic shells, it is likely that the results are more broadly applicable to other groups that form carbonate shells within the upper water column. For example, calcareous shells, such as ostracods, planktic foraminifera, and coccolithophores, are likely also impacted by the degradation of organic matter, both from decay of cellular material within their shells and from other organic matter in the water column (Lohmann, 1995; Schiebel et al., 2007; Monticelli Petró et al., 2018).

5. Conclusions

Decay experiments provide a window into the taphonomic process. Results from two experiments highlight that the oxidation of the internal organic body of the pteropod after death has a greater control over the dissolution of the shell than the aragonite saturation of the surrounding seawater. The amount of dissolution increased as the duration of the decay period increased. Conservatively, 10% of the total shell volume is removed due to this process on the timescales of 3.5–13 days, but this value is likely much higher due to increased shell porosity. This explanation for postmortem shell dissolution above the saturation horizon provides new insight in the process regulating the export of carbonate from the surface to the deep ocean. These findings have implications for interpreting pteropod shell condition from sediment trap and fossil records, as the impact of internally driven, postmortem shell dissolution must be taken in to account.

Acknowledgments
The authors declare no conflicts of interest. The data presented in the figures are available in the supporting information. The reconstructed CT data are available on Dryad doi:10.5061/dryad.8ts30t5. This work was carried out as part of the Ecosystems programme at the British Antarctic Survey. The authors would like to thank the crew and scientists of cruises JR271 and JR15002 for making the sample collection and decay experiments possible. Thanks to J. Urbanski, W. Yetter, and the team at GE in Lewistown, PA, for help with CT scanning and to J. Anderson and W. Auker from the MCL lab at Penn State for help with the SEM. Thanks to M. Humphreys for help with carbonate chemistry calculations, J. Gardner for the carbonate chemistry measurement for the 3.5-day decay experiment, and S. Sandrini for help with carbonate chemistry analysis for the 13-day decay experiment. The authors thank one anonymous reviewer whose comments helped to improve the quality of the manuscript. R. L. O. received funding from the Ellis L. Yochelson Award, the Hiroshi and Koya Ohmoto Graduate Student Fellowship, and the Alley Family Graduate Scholarship to support this work. R. L. O. and T. J. B. received funding from the Deike Research Fellowship.

References

Almogi-Labin, A., Luz, B., & Duplessy, J.-C. (1986). Quaternary paleo-oceanography, pteropod preservation and stable-isotope record of the Red Sea. *Palaeogeography Palaeoclimatology Palaeoecology*, *57*(2-4), 195–211. https://doi.org/10.1016/0031-0182(86)90013-1

Bathmann, U. V., Noji, T. T., & von Bodungen, B. (1991). Sedimentation of pteropods in the Norwegian Sea in autumn. *Deep Sea Research Part A, Oceanographic Research Papers*, *38*(10), 1341–1360. https://doi.org/10.1016/0198-0149(91)90031-A

Bednaršek, N., Feely, R. A., Reum, J. C. P., Peterson, B., Menkel, J., Alin, S. R., & Hales, B. (2014). *Limacina helicina* shell dissolution as an indicator of declining habitat suitability owing to ocean acidification in the California Current Ecosystem. *Proceedings of the Royal Society B: Biological Sciences*, *281*, 20140123. https://doi.org/10.1098/rspb.2014.0123

Bergan, A. J., Lawson, G. L., Maas, A. E., & Wang, Z. A. (2017). The effect of elevated carbon dioxide on the sinking and swimming of the shelled pteropod Limacina retroversa. *ICES Journal of Marine Science*, 1–13. https://doi.org/10.1093/icesjms/fsx008

Berger, W. H. (1978). Deep-sea carbonate: Pteropod distribution and the aragonite compensation depth. *Deep-Sea Research Part II: Topical Studies in Oceanography*, *25*(5), 447–452. https://doi.org/10.1016/0146-6291(78)90552-0

Berner, R. A., Berner, E. K., & Keir, R. S. (1976). Aragonite dissolution of the Bermuda Pedestal: Its depth and geochemical significance. *Earth and Planetary Science Letters*, *30*(2), 169–178. https://doi.org/10.1016/0012-821X(76)90243-0

Broecker, W. S., & Peng, T.-H. (1982). *Tracers in the Sea*. Palisades, New York: Lamont–Dohery Geological Observatory.

Buitenhuis, E. T., le Quéré, C., Bednaršek, N., & Schiebel, R. (2019). Large contribution of pteropods to shallow $CaCO_3$ export. *Global Biogeochemical Cycles*, *33*, 458–468. https://doi.org/10.1029/2018GB006110

Collier, R., Dymond, J., Honjo, S., Manganini, S., Francois, R., & Dunbar, R. (2000). The vertical flux of biogenic and lithogenic material in the Ross Sea: Moored sediment trap observations 1996-1998. *Deep-Sea Research Part II: Topical Studies in Oceanography*, *47*(15-16), 3491–3520. https://doi.org/10.1016/S0967-0645(00)00076-X

Crenshaw, M. A. (1990). Biomineralisation mechanics. In J. G. Carter (Ed.), *Skeletal Biomineralisation: Patterns, Processes and Evolutionary Trends*, (Vol. 1, pp. 1–9). New York: Van Nostrand Reinhold.

Cubillas, P., Köhler, S., Prieto, M., Chaïrat, C., & Oelkers, E. H. (2005). Experimental determination of the dissolution rates of calcite, aragonite, and bivalves. *Chemical Geology*, *216*(1–2), 59–77. https://doi.org/10.1016/j.chemgeo.2004.11.009

Dickson, A. G. (1990). Standard potential of the reaction: AgCl (s) +12H_2 (g) = Ag(s) + HCl (aq), and the standard acidity constant of the ion HSO_4^- in synthetic sea water from 273.15 tp 318.15 K. *The Journal of Chemical Thermodynamics*, *22*(2), 113–127. https://doi.org/10.1016/0021-9614(90)90074-Z

Doube, M., Kłosowski, M. M., Arganda-Carreras, I., Cordelières, F. P., Dougherty, R. P., Jackson, J. S., et al. (2010). BoneJ: Free and extensible bone image analysis in ImageJ. *Bone*, *47*(6), 1076–1079. https://doi.org/10.1016/j.bone.2010.08.023

Edmond, J. M. (1970). High precision determination of titration of alkalinity and total CO_2 of seawater by potentiometric titration. *Deep-Sea Research Part I: Oceanographic Research Papers*, *17*, 737–750.

Gattuso, J.-P., Gao, K., Lee, K., Rost, B., & Schulz, K. G. (2010). Approaches and tools to manipulate the carbonate chemistry. In U. Riebesell, V. J. Fabry, L. Hansson, & J.-P. Gattuso (Eds.), *Guide to best practices for ocean acidification research and data reporting* (pp. 41–52). Luxembourg: Publications Office of the European Union.

Gerhardt, S., Groth, H., Rühlemann, C., & Henrich, R. (2000). Aragonite preservation in late Quaternary sediment cores on the Brazilian Continental Slope: Implications for intermediate water circulation. *International Journal of Earth Sciences*, *88*(4), 607–618. https://doi.org/10.1007/s005310050291

Gerhardt, S., & Henrich, R. (2001). Shell preservation of *Limacina inflata* (Pteropoda) in surface sediments from the Central and South Atlantic Ocean: A new proxy to determine the aragonite saturation state of water masses. *Deep-Sea Research Part I: Oceanographic Research Papers*, *48*(9), 2051–2071. https://doi.org/10.1016/S0967-0637(01)00005-X

Goyet, C., Beauverger, C., Brunet, C., & Poisson, A. (1991). Distribution of carbon dioxide partial pressure in surface waters of the Southwest Indian Ocean. *Tellus Series B: Chemical and Physical Meteorology*, *43*(1), 1–11. https://doi.org/10.1034/j.1600-0889.1991.00001.x

Grégorie, C. (1972). Structure of the Molluscan shell. In M. Florkin, & B. T. Scheer (Eds.), *Mollusca*, (pp. 45–102). New York: Chemical Zoology.

Haddad, G., & Droxler, A. (1996). Metastable $CaCO_3$ dissolution at intermediate water depths of the Caribbean and western North Atlantic: Implications for intermediate water circulation during the past 200,000 years. *Paleoceanography*, *11*(6), 701–716. https://doi.org/10.1029/96PA02406

Harper, E. M. (1997). The molluscan periostracum: An important constraint in bivalve evolution. *Palaeontology*, *40*(1), 71–97.

Hildebrand, T., & Rüegsegger, P. (1997). A new method for the model-independent assessment of thickness in three-dimensional images. *Journal of Microscopy*, *185*(1), 67–75. https://doi.org/10.1046/j.1365-2818.1997.1340694.x

Janssen, A. W. (2012). Late Quaternary to Recent holoplanktonic Mollusca (Gastropoda) from bottom samples of the eastern Mediterranean Sea: Systematics, morphology. *Bollettino Malacologico*, *48*, 1–105.

Janssen, A. W., King, C., & Steurbaut, E. (2011). Notes on the systematics, morphology and biostratigraphy of fossil holoplanktonic Mollusca, 21. Early and Middle Eocene (Ypresian-Lutetian) holoplanktonic Mollusca (Gastropoda) from Uzbekistan. *Basteria*, *75*(20), 71–93.

Janssen, A. W., & Peijnenburg, K. T. C. A. (2017). An overview of the fossil record of Pteropoda (Mollusca, Gastropoda, Heterobranchia). *Cainozoic Research*, *17*, 3–10.

Janssen, A. W., Sessa, J. A., & Thomas, E. (2016). Pteropoda (Mollusca, Gastropoda, Thecosomata) from the Paleocene-Eocene thermal maximum (United States Atlantic Coastal Plain). *Palaeontologia Electronica*, 1–26.

Keul, N., Peijnenburg, K. T. C. A., Andersen, N., Kitidis, V., Goetze, E., & Schneider, R. R. (2017). Pteropods are excellent recorders of surface temperature and carbonate ion concentration. *Scientific Reports*, *7*(1), 1–11. https://doi.org/10.1038/s41598-017-11,708-w

Lalli, C. M., & Gilmer, R. W. (1989). *Pelagic Snails*. Stanford: Stanford University Press.

Lavigne, H., Epitalon, J.-M., & Gattuso, J.-P. (2011). seacarb:seawater carbonate chemistry with R.

Lee, K., Tong, L. T., Millero, F. J., Sabine, C. L., Dickson, A. G., Goyet, C., et al. (2006). Global relationships of total alkalinity with salinity and temperature in surface waters of the world's oceans. *Geophysical Research Letters*, *33*, L19605. https://doi.org/10.1029/2006GL027207

Lohmann, G. P. (1995). A model for variation in the chemistry of planktonic foraminifera due to secondary calcification and selective dissolution. *Paleoceanography*, *10*(3), 445–457. https://doi.org/10.1029/95PA00059

Manno, C., Bednaršek, N., Tarling, G. A., Peck, V. L., Comeau, S., Adhikari, D., et al. (2017). Shelled pteropods in peril: Assessing vulnerability in a high CO_2 ocean. *Earth-Science Reviews*, *169*, 132–145. https://doi.org/10.1016/j.earscirev.2017.04.005

Manno, C., Sandrini, S., Tositti, L., & Accornero, A. (2007). First stages of degradation of *Limacina helicina* shells observed above the aragonite chemical lysocline in Terra Nova Bay (Antarctica). *Journal of Marine Systems*, *68*(1–2), 91–102. https://doi.org/10.1016/j.jmarsys.2006.11.002

Martin, W. R., & Sayles, F. L. (1996). $CaCO_3$ dissolution in sediments of the Ceara Rise, western equatorial Atlantic. *Geochimica et Cosmochimica Acta*, *60*(2), 243–263. https://doi.org/10.1016/0016-7037(95)00383-5

Mehrbach, C., Culberson, C. H., Hawley, J. E., & Pytkowicz, R. M. (1973). Measurement of the apparent dissociation constants of carbonic acid in seawater at atmospheric pressure. *Limnology and Oceanography*, *18*(6), 897–907. https://doi.org/10.4319/lo.1973.18.6.0897

Meinecke, G., & Wefer, G. (1990). Seasonal pteropod sedimentation in the Norwegian Sea. *Palaeogeography Palaeoclimatology Palaeoecology*, *79*(1–2), 129–147. https://doi.org/10.1016/0031-0182(90)90109-K

Melzner, F., Stange, P., Trubenbach, K., Thomsen, J., Casties, I., Panknin, U., et al. (2011). Food supply and seawater pCO_2 impact calcification and internal shell dissolution in the blue mussel *Mytilus edulis*. *PLoS ONE*, *6*(9). https://doi.org/10.1371/journal.pone.0024223

Milliman, J. D., & Droxler, A. W. (1996). Neritic and pelagic carbonate sedimentation in the marine environment: ignorance is not bliss. *Geologische Rundschau*, *85*(3), 496–504. https://doi.org/10.1007/BF02369004

Milliman, J. D., Troy, P. J., Balch, W. M., Adams, A. K., Li, Y., & Mackenzie, F. T. (1999). Biologically mediated dissolution of calcium carbonate above the chemical lysocline? *Deep-Sea Research Part I: Oceanographic Research Papers*, *46*(10), 1653–1669. https://doi.org/10.1016/S0967-0637(99)00034-5

Mohan, R., Verma, K., Mergulhao, L. P., Sinha, D. K., Shanvas, S., & Guptha, M. V. S. (2006). Seasonal variation of pteropods from the Western Arabian Sea sediment trap. *Geo-Marine Letters*, *26*(5), 265–273. https://doi.org/10.1007/s00367-006-0035-1

Monticelli Petró, S., do Nacimento Ritter, M., Gómez Pivel, M. A., & Comibra, J. C. (2018). Surviving in the water column: Defining the taphonomically active zone in pelagic systems. *Palaios*, *33*(3), 85–93. https://doi.org/10.2110/palo.2017.032

Mucci, A. (1983). The solubility of calcite and aragonite in seawater at various salinities, temperatures, and one atmosphere total pressure. *American Journal of Science*, *283*(7), 780–799. https://doi.org/10.2475/ajs.283.7.780

Oakes, R. L., Peck, V. L., Manno, C., & Bralower, T. (2019). Impact of preservation techniques on pteropod shell condition. *Polar Biology*, *42*(2), 257–269. https://doi.org/10.1007/s00300-018-2419-x

Olsen, A., Key, R. M., van Heuven, S., Lauvset, S. K., Velo, A., Lin, X., et al. (2016). The global ocean data analysis project version 2 (GLODAPv2) - An internally consistent data product for the world ocean. *Earth System Science Data*, *8*(2), 297–323. https://doi.org/10.5194/essd-8-297-2016

Peck, V. L., Tarling, G. A., Manno, C., & Harper, E. M. (2016). Response to comment. *Deep-Sea Research Part II: Topical Studies in Oceanography*, *81-84*, 102–113. https://doi.org/10.1016/j.dsr2.2011.05.004

Peck, V. L., Tarling, G. A., Manno, C., Harper, E. M., & Tynan, E. (2016). Outer organic layer and internal repair mechanism protects pteropod *Limacina helicina* from ocean acidification. *Deep-Sea Research Part II: Topical Studies in Oceanography*, *127*, 41–52. https://doi.org/10.1016/j.dsr2.2015.12.005

Pierrot, D., E. Lewis, & D. W. R. Wallace (2006). MS Excel program developed for CO2 system calculations. https://doi.org/10.3334/CDIAC/otg.CO2SYS_XLS_CDIAC105a

Roberts, D., Howard, W. R., Moy, A. D., Roberts, J. L., Trull, T. W., Bray, S. G., & Hopcroft, R. R. (2011). Interannual pteropod variability in sediment traps deployed above and below the aragonite saturation horizon in the Sub-Antarctic Southern Ocean. *Polar Biology*, *34*(11), 1739–1750. https://doi.org/10.1007/s00300-011-1024-z

Sato-Okoshi, W., Okoshi, K., Sasaki, H., & Akiha, F. (2010). Shell structure of two polar pelagic molluscs, Arctic *Limacina helicina* and Antarctic *Limacina helicina antarctica* forma antarctica. *Polar Biology*, *33*(11), 1577–1583. https://doi.org/10.1007/s00300-010-0849-1

Schiebel, R. (2002). Planktic foraminiferal sedimentation and the marine calcite budget. *Global Biogeochemical Cycles*, *16*(4), 1065. https://doi.org/10.1029/2001GB001459

Schiebel, R., Barker, S., Lendt, R., Thomas, H., & Bollmann, J. (2007). Planktic foraminiferal dissolution in the twilight zone. *Deep-Sea Research Part II: Topical Studies in Oceanography*, *16*(4), 3-1–3-21. https://doi.org/10.1029/2001GB001459

Schneider, C. A., Rasband, W. S., & Eliceiri, K. W. (2012). NIH Image to ImageJ: 25 years of image analysis. *Nature Methods*, *9*(7), 671–675. https://doi.org/10.1038/nmeth.2089

Tunnicliffe, V., Davies, K. T. A., Butterfield, D. A., Embley, R. W., Rose, J. M., & Chadwick, W. W. Jr. (2009). Survival of mussels in extremely acidic waters on a submarine volcano. *Nature Geoscience*, *2*(5), 344–348. https://doi.org/10.1038/ngeo500

Tynan, E., Clarke, J. S., Humphreys, M. P., Ribas-Ribas, M., Esposito, M., Rérolle, V. M. C., et al. (2016). Physical and biogeochemical controls on the variability in surface pH and calcium carbonate saturation states in the Atlantic sectors of the Arctic and Southern Oceans. *Deep-Sea Research Part II: Topical Studies in Oceanography*, *127*, 7–27. https://doi.org/10.1016/j.dsr2.2016.01.001

Wall-Palmer, D., Hart, M. B., Smart, C. W., Sparks, R. S. J., Le Friant, A., Boudon, G., et al. (2012). Pteropods from the Caribbean Sea: Variations in calcification as an indicator of past ocean carbonate saturation. *Biogeosciences*, *9*(1), 309–315. https://doi.org/10.5194/bg-9-309-2012

Wall-Palmer, D., Smart, C. W., & Hart, M. B. (2013). In-life pteropod shell dissolution as an indicator of past ocean carbonate saturation. *Quaternary Science Reviews*, *81*, 29–34. https://doi.org/10.1016/j.quascirev.2013.09.019